

Letter

Nuclear quadrupole moments of $5/2^-$ and $9/2^-$ states in ^{169}Ta

Vivek Kumar¹, P. Thakur¹, A.K. Bhati^{1,a}, R.P. Singh², and R.K. Bhowmik²

¹ Centre for Advanced Studies in Physics, Panjab University, Chandigarh-160 014, India

² Inter-University Accelerator Centre, JNU Campus, New Delhi-110 067, India

Received: 17 July 2005 / Revised version: 7 December 2005 /

Published online: 27 December 2005 – © Società Italiana di Fisica / Springer-Verlag 2005

Communicated by D. Schwalm

Abstract. The nuclear spectroscopic quadrupole moments for the $\pi h_{9/2}5/2^-, 1/2^- [541]$ and the $\pi h_{11/2}9/2^-, 9/2^- [514]$ isomeric states in ^{169}Ta have been measured employing the time differential perturbed angular-distribution technique following the nuclear reaction $^{159}\text{Tb}(^{16}\text{O}, 6n\gamma)^{169}\text{Ta}$ at beam energy 104 MeV. The ratio of the intrinsic quadrupole moments $Q_0(K^\pi = 5/2^-)/Q_0(K^\pi = 9/2^-)$ has been derived as 1.87(13) from the measured quadrupole precession frequencies of the corresponding states. The model-independent analysis of the equilibrium deformation indicates strong prolate- and oblate-driving nature of the $1/2^- [541]$ and $9/2^- [514]$ orbitals in $^{169,171}\text{Ta}$ isotopes, respectively.

PACS. 21.10.Hw Spin, parity, and isobaric spin – 21.10.Ky Electromagnetic moment – 27.70.+q $150 \leq A \leq 189$

The ground states in odd-even $^{171,173}\text{Ta}$ nuclei are established as $\pi 5/2^-, 1/2^- [541]$ Nilsson configuration [1] but in the case of neighbouring nuclei $^{167,169}\text{Ta}$, there is ambiguity in the assignment of low-lying proton intrinsic states because of missing inter-band transitions [2,3]. The identification of the band heads and the rotational bands built on them is based on the in-band analysis and the systematics of the transitional energies in neighbouring nuclei. Zhang *et al.* [4] have observed two isomeric band heads $I = 5/2^-$ ($E_x = (169.5 + x)$ keV, $T_{1/2} = 17(4)$ ns) and $I = 9/2^-$ ($E_x = 220$ keV, $T_{1/2} = 28(5)$ ns) of the $1/2^- [541]$ and $9/2^- [514]$ bands in ^{169}Ta , respectively. Transitions to the lower level are still uncertain. Both the rotational bands belong to the high- j proton configurations having different deformation-driving forces. Guided by these facts, it was decided to measure the spectroscopic quadrupole moments of the isomeric levels using the time differential perturbed angular-distribution (TDPAD) technique to confirm the spin of the levels unambiguously and to provide directly the configuration dependence of deformation.

The TDPAD measurements were carried out at the 16UD Pelletron accelerator facility of the Inter-University Accelerator Centre, New Delhi. The $5/2^-$ and $9/2^-$ isomeric states were excited through the nuclear reaction $^{159}\text{Tb}(^{16}\text{O}, 6n\gamma)^{169}\text{Ta}$ using 104 MeV ^{16}O pulsed beam

with 1 μs repetition period. The target consisted of a 2 mg/cm² thick Tb metal foil just enough to stop the recoiling Ta nuclei. The details of the TDPAD setup are given elsewhere [5]. The de-exciting γ -rays from the isomeric levels were detected in two NaI(Tl) detectors ($3'' \times 2''$ crystals coupled to the RCA 8575 low noise photomultiplier tubes) placed at 0° and 90° with respect to the beam direction at a distance of 20 cm from the target. The time signal was generated by the time-to-amplitude converter (TAC) started by a suitably shaped anode pulse of NaI(Tl) detector and stopped by a pulse picked up from the main oscillator of the pulsing system. For faster data acquisition the prompt peak was suppressed and the low-energy part of the spectrum (unresolved X-rays and γ -rays) had to be cut off. The data were collected in LIST mode with four parameters: the energy and time signals for both NaI(Tl) detectors. The acquired data, following proper gain matching for energy and time, were sorted off-line into E_γ - t matrices corresponding to the two different detectors. In order to investigate the delayed gamma rays produced in the reaction, energy spectra gated at different time intervals with respect to the beam pulses were created. The delayed γ -ray energy spectra using the NaI(Tl) and the HPGe detectors are shown in fig. 1. The HPGe detector was used only to identify the de-exciting γ -rays. The high background at low energy has been observed due to short-lived residual radioactivities. The background-subtracted normalised time spectra

^a e-mail: akbhati@pu.ac.in

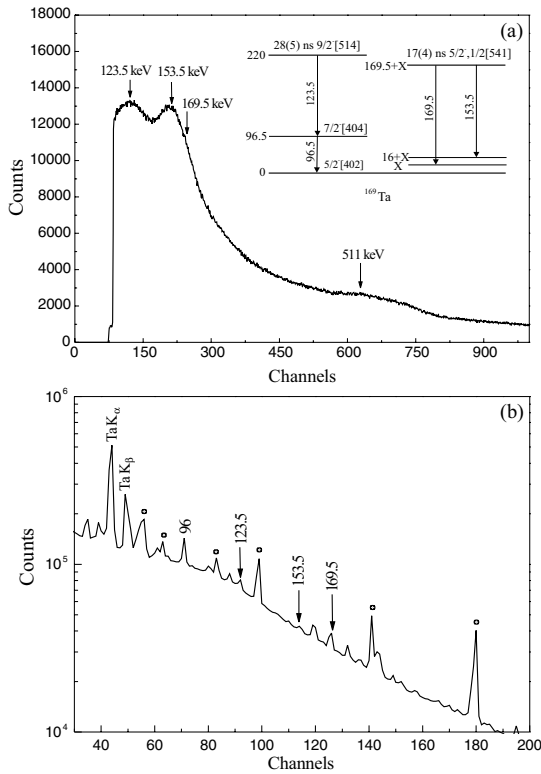


Fig. 1. The partial level scheme of ^{169}Ta at low excitations [4] and the delayed γ -ray spectrum observed by (a) NaI(Tl) and (b) HGe without background subtraction.

at 0° and 90° for the corresponding isomeric states were added together to further ascertain the isomeric character of the 123.5, 153.5 and 169.5 keV γ -rays. The half-lives $T_{1/2}(5/2^-) = 44(5)$ ns and $T_{1/2}(9/2^-) = 54(6)$ ns have been derived from the least-squares (LSQ) fitting of the time spectra plotted in fig. 2. The derived values of the half-lives are higher compared to the earlier reported values [4] obtained through γ - γ coincidence to avoid contaminants. Further, the TDPAD patterns, analysed below for the de-exciting γ -rays, depend only on the spin of the isomeric states and are different for the $5/2^-$ and $9/2^-$ isomeric states (figs. 3 and 4).

The recoiling ^{169}Ta nuclei get implanted into Tb metal backing in the paramagnetic phase at room temperature (300 K) and experience only the electric quadrupole interaction because of its hexagonal close packed lattice structure. The transition from the paramagnetic phase to the magnetic ordered state in Tb metal takes place at 229 K (Néel temperature). The γ -ray angular distribution, perturbed by the electric quadrupole interactions, results in the time-dependent modulation of the γ -ray intensities. From the measured intensities, a ratio function $G_{22}(t)$ was formed,

$$G_{22}(t) = \frac{2}{A_{22}} \left[\frac{I(0^\circ, t) - I(90^\circ, t)}{I(0^\circ, t) + 2I(90^\circ, t)} \right]. \quad (1)$$

Here $I(\theta, t)$ are the background-subtracted and normalized time spectra at two angles 0° and 90° . The experimental ratio functions $G_{22}(t)$ for each isomeric state were

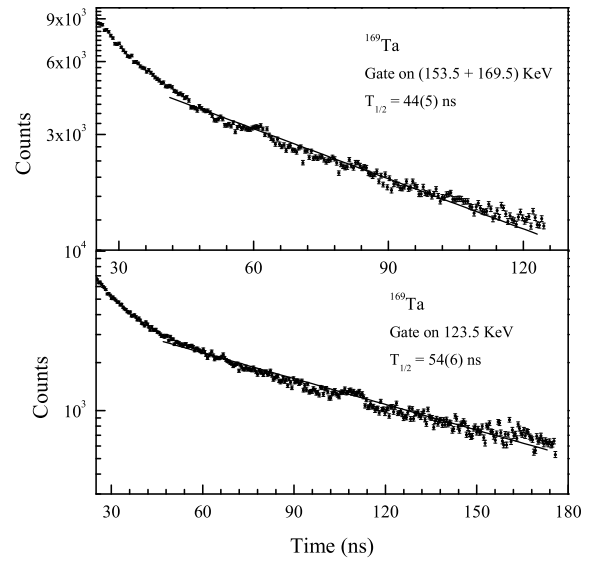


Fig. 2. Summed time spectra for the $5/2^-$ and the $9/2^-$ isomeric states.

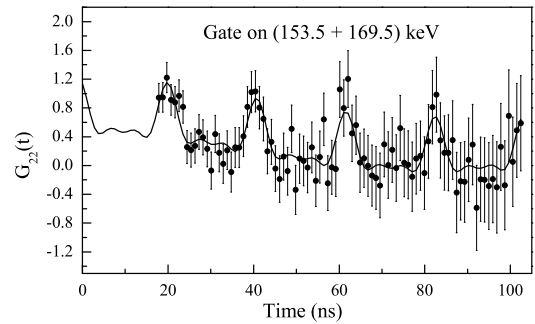


Fig. 3. Spin rotation spectrum of the $5/2^-$ state in ^{169}Ta .

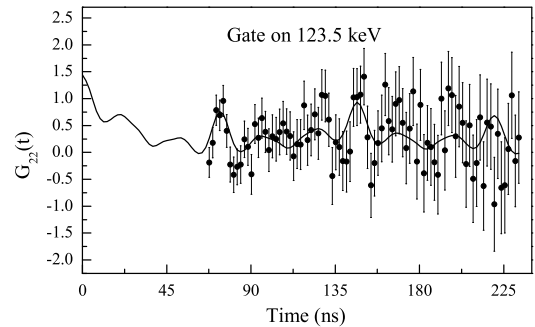


Fig. 4. Spin rotation spectrum of the $9/2^-$ state in ^{169}Ta .

least-squares fitted to the following theoretical perturbation function for two sites in a polycrystalline material:

$$G_{22}(t) = f \sum S_{2n} \cos(n\omega_0 t) \times \exp \left[-\frac{1}{2} (n\delta\omega_0 t)^2 \right] + (1-f) \sum S_{2n} \cos(n\omega_0 t) \times \exp \left[-\frac{1}{2} (n\delta'\omega_0 t)^2 \right], \quad (2)$$

Table 1. Comparison of the deformation parameters $\beta_2^*(\text{exp.})$ and the crossing frequencies in $^{169,171}\text{Ta}$.

Nucleus	Rotational band	$\beta_2(\text{TRS})^{(a)}$	$\beta_2(\text{Th.})$	$\beta_2^*(\text{exp.})$	$\hbar\omega_c$ MeV	$\Delta\beta_2^*(\text{exp.})^{(b)}$	$\Delta\hbar\omega_c^{(c)}$ MeV
^{169}Ta	$5/2^-$	0.256	0.256	0.275	0.31	0.046	-0.05
	$9/2^-$	0.245	0.216	0.147	0.24	-0.082	0.02
^{171}Ta	$5/2^-$	0.26	0.267	0.24	0.29	0.0	-0.015
	$9/2^-$		0.234	0.198	0.26	-0.04	0.015
^{168}Hf	yrast		0.246	0.229	0.26		
^{170}Hf	yrast		0.260	0.244	0.275		

(a) Refs. [3, 7].

(b) The change in the observed deformation $\Delta\beta_2^*(\text{exp.}) = \beta_2(\text{exp.})(^{169,171}\text{Ta}) - \beta_2(\text{exp.})(^{168,170}\text{Hf})$.(c) The shift in the crossing frequency $\Delta\hbar\omega_c = \hbar\omega_c(^{168,170}\text{Hf}) - \hbar\omega_c(^{169,171}\text{Ta})$.

where the symbols have their usual meaning. The least-squares fitting of the data has been explained in detail in ref. [5]. The fractions f and $(1-f)$ correspond to the recoil-implanted nuclei at the regular substitutional and the irregular sites, respectively. The nuclei at the substitutional sites are characterised by the unique axially symmetric (asymmetry parameter $\eta = 0$) electric field gradient (efg) associated with the interaction frequency (ω_{01}) with small distribution (δ), while nuclei at irregular sites experience low quadrupole interaction frequency (ω_{02}) with broad distribution (δ'). The amplitude of the modulation is determined by the effective anisotropy contribution of $(153.5 + 169.5)$ keV γ -ray transitions for the $5/2^-$ state and 123.5 keV γ -ray transitions for the $9/2^-$ state.

For the $5/2^-$ state, the solid line shown in fig. 3 represents a fitted quadrupole interaction pattern with parameters $\omega_{01} = 301.2(12)$ Mrad/s and $\omega_{02} = 19.9(4)$ Mrad/s corresponding to the regular and irregular sites, respectively. In the case of the $9/2^-$ state, the solid line shown in fig. 4 corresponds to the interaction frequencies $\omega_{01} = 85.8(6)$ Mrad/s and $\omega_{02} = 9.1(2)$ Mrad/s. The fraction (f) and field distribution (δ) at regular sites are observed to be 70% and 0.01, respectively, for both the isomeric states. The quadrupole interaction frequencies at the irregular sites are low and are not sensitive to the distribution in the LSQ fitting. The shape of the quadrupole precession pattern confirms unambiguously the spin values $I = 5/2^-$ and $I = 9/2^-$ for the corresponding band heads.

For half-integer spin, the quadrupole interaction frequency ω_{01} is related to the spectroscopic quadrupole moment Q_s and the electric field gradient V_{zz} through the relation

$$\omega_{01} = \frac{6eQ_s V_{zz}}{4I(2I-1)\hbar}. \quad (3)$$

Using the measured value of $V_{zz} = 593(35) \times 10^{15}$ V/cm² at ^{181}Ta [6] in Tb at room temperature and the LSQ-fitted values of ω_{01} for the substitutional sites, the extracted values of Q_s are found to be $Q_s(5/2^-) = 2.23(13)$ b and $Q_s(9/2^-) = 2.28(13)$ b. The electric field gradient measurements for the implanted and the molten $^{181}\text{TaTb}$ sources have shown the same value at the substitutional sites [6]. The fraction of the ions going to the substitutional sites and the slow interaction frequency component

(due to radiation damage and light impurity ions trapping at the irregular sites) is influenced by the sample preparation techniques.

The spectroscopic quadrupole moment Q_s is related to the intrinsic quadrupole moment Q_0 by the relation,

$$Q_s = Q_0 \frac{3K^2 - I(I+1)}{(I+1)(2I+3)} \quad (4)$$

The values of Q_0 for the $5/2^-$ and $9/2^-$ isomeric states obtained by using the above relation turn out to be 7.80(45) b and 4.18(24) b, respectively, and the ratio of the two intrinsic quadrupole moments is $Q_0(5/2^-)/Q_0(9/2^-) = 1.87(13)$. The ratio of the intrinsic quadrupole moments is free from any systematic uncertainty in the value of the electric field gradient at the nucleus. From the measured quadrupole moment values, $Q_0(5/2^-) = 6.69$ [7] and $Q_0(9/2^-) = 5.66(34)$ [5] in ^{171}Ta , it is observed that with the decrease of the neutron number in the $^{169,171}\text{Ta}$ isotopes, the intrinsic quadrupole moment of the $5/2^-$ band head increases [$Q_0(^{169}\text{Ta})/Q_0(^{171}\text{Ta}) = 1.77(7)$] by 17% and that of the $9/2^-$ band head decreases [$Q_0(^{169}\text{Ta})/Q_0(^{171}\text{Ta}) = 0.74(6)$] by 25%. This is the first direct observation of such a large variation in the quadrupole deformation for the two different configurations in a nucleus and also in two neighbouring isotopes. The results are compared with the available theoretical predictions below.

As a good estimate, the equilibrium quadrupole deformation β_2 can be evaluated from the relation

$$Q_0 = \frac{4ZR^2\beta_2 \cos \gamma}{5}, \quad (5)$$

where Z is the atomic number, $R = R_0A^{1/3}$ and $R_0 = 1.2$ fm. The calculated values of the corresponding deformation parameters for the axially symmetric shape are $\beta_2(5/2^-) = 0.303(17)$ and $\beta_2(9/2^-) = 0.162(9)$. The sign of the quadrupole moment cannot be found in the present experiment, but we can take it to be positive (prolate) based on the measurements for the $5/2^-$ and the $9/2^-$ band heads in ^{173}Ta [8] and ^{181}Ta [9], respectively. There are indications of small deviations from the axial symmetry (*i.e.* β - and γ -deformation) from the observation of the

energy signature splitting in the one-quasiproton bands (comparatively larger in the $9/2^-$ band). For the light odd-mass Ta isotopes the increased amplitude of the signature splitting in the $9/2^-$ band with decreasing neutron number (N) has been attributed to the non-axially symmetric shapes [10]. The stiffness to the γ -distortion goes down fast below $N = 104$. The total-Routhian-surface (TRS) calculations based on a Woods-Saxon deformed potential have predicted small negative γ -deformation ($\gamma < 4^\circ$) in ^{169}Ta [3]. The extracted deformation parameter, β_2 , is related to the charge distribution and is divided by 1.1 to transform it to the quadrupole deformation of the Woods-Saxon mean field [11] (sensitive to the nuclear matter distribution), $\beta_2^*(\text{exp.})$, calculated by Nazarewicz *et al.* [12]. Both the experimental and the theoretical results for $^{169,171}\text{Ta}$ isotopes are reported in table 1. For comparison, the deformation parameters of the even-even core $^{168,170}\text{Hf}$ nuclei [12] have also been included.

The results show that i) the equilibrium deformation associated with the $5/2^-$ band head is larger (approximately twice as large) compared to that with the $9/2^-$ band head and ii) the change in the deformation for the corresponding states in ^{169}Ta is approximately equal and in the opposite direction (increasing for the $5/2^-$ state and decreasing for the $9/2^-$ state) with respect to the ^{171}Ta isotope. This agrees qualitatively with the theoretical predictions for the deformation change in odd- Z rare-earth nuclei [12]. The variation in the induced deformation (nuclear shape) in the core is attributed to the different deformation-driving forces of the single-quasiproton orbitals. The $\pi 1/2^-$ [541] orbital is characterised by the large negative slope ($\partial\epsilon/\partial\beta < 0$) in the Nilsson diagram and is known as strongly prolate-driving orbital. The occupation of the orbital by the proton strongly favours the prolate deformation of the core. The $\pi 9/2^-$ [514] orbital has positive slope ($\partial\epsilon/\partial\beta > 0$) and is an oblate-driving orbital. The occupation of this orbital results in favour of a less-prolate-shape core. The configuration-dependent core polarisation effects can give a difference in the deformation parameter for the $5/2^-$ and the $9/2^-$ isomers in ^{169}Ta and across other odd Ta isotopes. The ^{169}Ta isotope is nearer to the transitional region, comparatively large deformation spread is expected in it due to the core softness towards γ -deformation [12]. The variation in magnitude and direction is at variance with the theoretical computed values. The occupation of the single-proton orbital influences the first crossing frequency of the band due to the alignment of the pair of $i_{13/2}$ neutrons also through the configuration-dependent deformation effects. The shift in the crossing frequencies between the $1/2^-$ [541] and the $9/2^-$ [514] sequences in the $^{169,171}\text{Ta}$

isotopes and the corresponding $^{168,170}\text{Hf}$ [13,14] even-even yrast sequences (table 1) seems to be related with the change in deformation, in magnitude and direction. The observed crossing frequency shifts across the odd Ta isotopic chain could not be reproduced by the cranked-shell calculations with the deformation parameters obtained from the TRS calculations [15]. The shift is reproduced by considering quadrupole pairing in the projected shell model [16] and the filling of certain neutron shell is important. The static quadrupole moment measurements for the $5/2^-$ and the $9/2^-$ isomers occurring in other odd Ta isotopes can elucidate the role of other related factors for the AB-crossing frequencies.

The theoretical calculations of the deformation parameter [12] are based on the pure single-quasiparticle nature of the state. The deviation from the theoretical predictions is expected because of other microscopic details of the wave functions of the single-particle states, *e.g.* K -mixing, coupling of octupole vibrations etc., which have not been included here. The sign of the quadrupole moment cannot be measured in the present experiment, which restricts the determination of the nature of the quadrupole deformation. We plan to perform g -factor measurements in ^{169}Ta to know the precise nature of the states.

The authors wish to thank the accelerator crew, particularly Mr S. Chopra and Mr R. Joshi for the stable beam at the Inter-University Accelerator Centre during the experiment. One of us (V.K.) acknowledges the financial assistance from the UGC/IUAC.

References

1. B. Harmatz *et al.*, Phys. Rev. C **12**, 1083 (1975).
2. K. Theine *et al.*, Nucl. Phys. A **536**, 418 (1992).
3. S.G. Li *et al.*, Nucl. Phys. A **555**, 435 (1993).
4. Y.H. Zhang *et al.*, Eur. Phys. J. A **1**, 1 (1998).
5. R. Dogra *et al.*, Hyperfine Interact. **96**, 223 (1995).
6. M. Forker *et al.*, Hyperfine Interact. **9**, 255 (1981).
7. P. Joshi *et al.*, Phys. Rev. C **60**, 034311 (1999).
8. R. Eder *et al.*, Phys. Lett. B **133**, 44 (1983).
9. M. Eibschütz *et al.*, Phys. Lett. A **93**, 259 (1983).
10. M.S. Fetea *et al.*, Nucl. Phys. A **690**, 239c (2001).
11. J. Dudek *et al.*, Nucl. Phys. A **420**, 285 (1984).
12. W. Nazarewicz *et al.*, Nucl. Phys. A **512**, 61 (1990).
13. R. Chapman *et al.*, Phys. Rev. Lett. **51**, 2265 (1983).
14. J.C. Lisle *et al.*, Nucl. Phys. A **366**, 281 (1981).
15. C.H. Yu *et al.*, Nucl. Phys. A **511**, 157 (1990).
16. Y. Sun *et al.*, Phys. Rev. Lett. **72**, 3483 (1994).